Rustrela Virus in Wild Mountain Lion (*Puma concolor*) with Staggering Disease, Colorado, USA

Karen A. Fox, Angele Breithaupt, Martin Beer, Dennis Rubbenstroth, Florian Pfaff

We identified a rustrela virus variant in a wild mountain lion (*Puma concolor*) in Colorado, USA. The animal had clinical signs and histologic lesions compatible with staggering disease. Considering its wide host range in Europe, rustrela virus should be considered as a cause for neurologic diseases among mammal species in North America.

On May 12, 2023, Colorado Parks and Wildlife (Denver, CO, USA) received a report of an ≈1-year-old free-ranging female mountain lion (*Puma concolor*) with signs of severe hind leg ataxia and paresis. The lion had been observed in a residential area of Douglas County, Colorado, USA (Appendix Figure 1, https://wwwnc.cdc.gov/EID/article/30/8/24-0411-App1.pdf). The animal was reluctant to rise and had markedly decreased capacity to move or bear weight on the hind end (Video, https://wwwnc.cdc.gov/EID/article/30/8/24-0411-V.htm). The animal appeared depressed but was still responsive to stimuli. Wildlife officers tranquilized the animal and then euthanized it by gunshot to the chest to prevent destruction of neurologic tissues. We conducted a postmortem investigation including necropsy, histopathology, immunohistochemistry, molecular diagnostics, and metatranscriptome sequencing to investigate potential causes of the disease.

The Study

Prenecropsy radiology revealed no skeletal abnormalities to explain the clinical signs observed. Necropsy results indicated poor body condition and mild bruising at the torso and limbs. The stomach contained only pine needles. Histopathology demonstrated severe nonsuppurative meningoencephalomyelitis (Appendix). The leptomeninges were multifocally and markedly expanded by lymphocytes and histiocytes in both brain and spinal cord (Figure 1). Virchow-Robin perivascular spaces were expanded by dense cuffs of lymphocytic to lymphohistiocytic infiltrates up to 20 cell layers thick in nearly all regions of the brain (Figure 1, panels A–C) and spinal cord. Inflammation was largely restricted to the leptomeninges and gray matter, and only minimal in the white matter (Figure 1, panels A, B). Affected sections also demonstrated scattered neuronal necrosis, gliosis, and loose glial nodules (Figure 1, panels B, E, G), partially leading to an irregular architecture (Figure 1, panel G). The cerebellar cortex showed no indication of inflammation or degenerative process (Figure 1, panel I)

Initial diagnostic tests did not detect feline panleukopenia virus, canine distemper virus, West Nile virus, *Toxoplasma gondii*, influenza A virus, rabies virus, or feline infectious peritonitis virus in the central nervous system (Appendix Table 1). We used pooled brain and spinal cord tissue to extract total RNA (Appendix), then conducted metatranscriptome sequencing to obtain sequence fragments (reads). We used those fragments to de novo assemble a single contiguous sequence (contig) with homology to known sequences of rustrela virus (RusV). The contig represented the whole viral genome and matched RusV reference strains. We submitted the annotated RusV genome sequence to the International Nucleotide Sequence Database Collaboration (https://www.insdc.org; accession no. PP025855).

We adapted real-time reverse transcription PCR primers and probe for RusV (*1*) by using degenerate bases for consensus homology to the Colorado mountain lion–derived sequence and European RusV sequences (Appendix Table 2). Those adapted methods

Author affiliations: Colorado State University College of Veterinary Medicine and Biomedical Sciences, Fort Collins, Colorado, USA (K.A. Fox); Colorado Parks and Wildlife, Fort Collins (K.A. Fox); Friedrich-Loeffler-Institut, Greifswald-Insel Riems, Germany (A. Breithaupt); Institute of Diagnostic Virology, Friedrich-Loeffler-Institut, Greifswald-Insel Riems (M. Beer, D. Rubbenstroth, F. Pfaff)

DOI: https://doi.org/10.3201/eid3008.240411

showed RusV RNA in a pooled sample of brain and spinal cord from the mountain lion, with a cycle threshold value of 20.3.

RusV (*Rubivirus strelense*), a member of the family *Matonaviridae*, was recently identified as the cause of staggering disease (*1*), a usually fatal neurologic syndrome in cats. Since the 1970s, staggering disease has been documented in domestic cats in Europe, predominantly in Sweden and Austria (*2*–*6*). Affected cats show a consistent combination of histologic lesions and clinical signs, including hind limb ataxia or paresis, and nonsuppurative meningoencephalitis

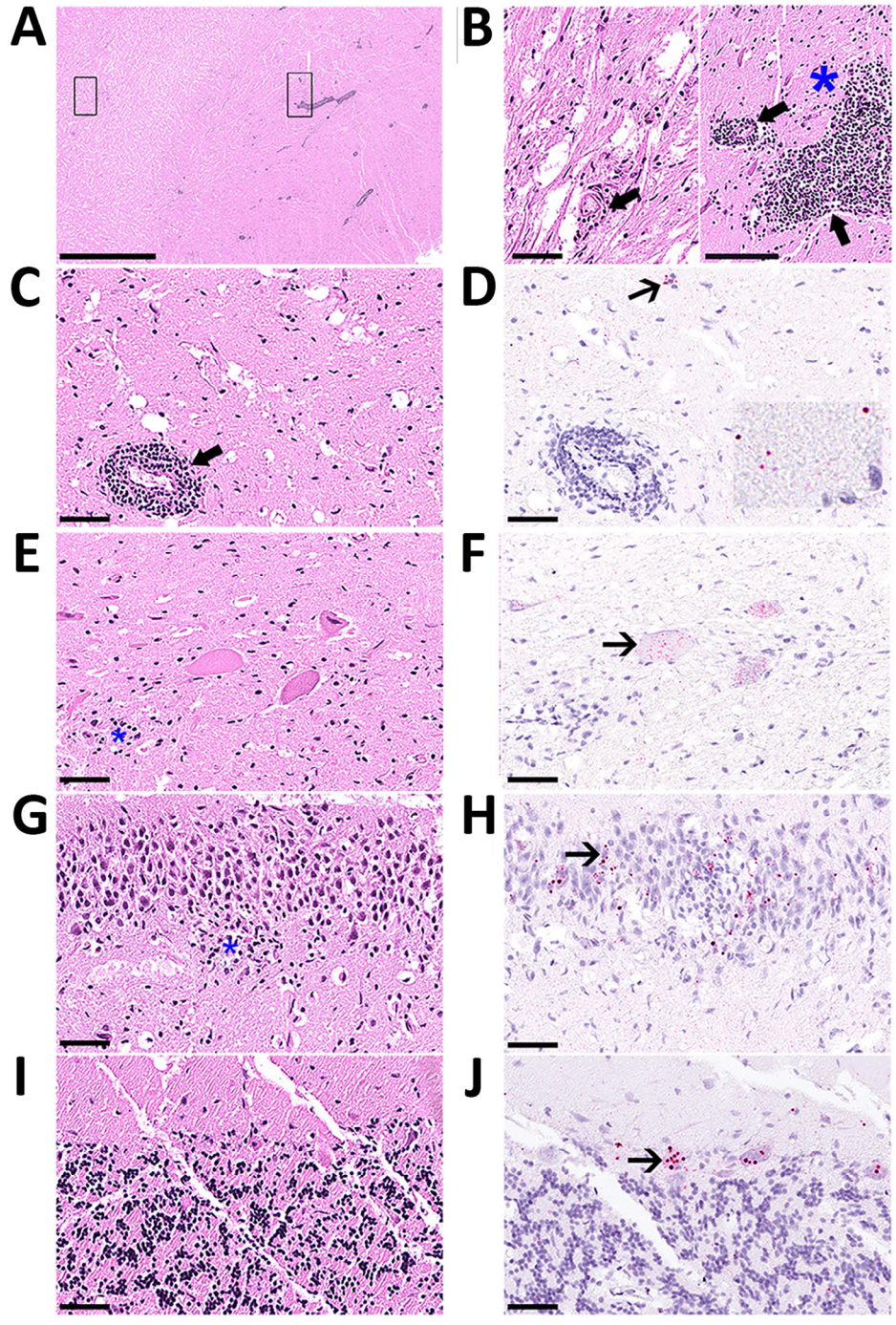

Figure 1. Histology of brain and spinal cord used to detect rustrela virus (RusV) in wild mountain lion (*Puma concolor*) with staggering disease, Colorado, USA. RusV RNA was detected by RNAscope Reagent Kit-Red (Advanced Cell Diagnostics/bio-techne, https://www.bio-techne.com) in situ hybridization. All sections demonstrate artifactual clefting of the neuropil due to freezing of the tissue postmortem. A) Cerebral cortex with perivascular cuffing and mild gliosis of the white and gray matter; boxes indicate detailed areas in panel B. Scale bar indicates 2.5 mm. B) The white matter (left panel) is minimally affected by perivascular lymphohistiocytic infiltrates (bold arrow), compared with the gray matter (right panel), also showing gliosis (asterisk). Scale bar indicates 100 µm. C) Midbrain affected by perivascular cuffing. Scale bar indicates 50 µm. D) Midbrain showing chromogenic labeling (fast red) of RusV in neuronal cell bodies (slender arrow) and in the neuropil (inlay). Scale bar indicates 50 µm. E) Spinal cord with 3 motor neurons showing variable degree of degeneration/necrosis and also gliosis (asterisk). Scale bar indicates 50 µm. F) Spinal cord with affected motor neurons with RusV RNA detection. Scale bar indicates 50 µm. G) Hippocampus exhibiting irregular architecture of the granule layer and gliosis (asterisk). Scale bar indicates 50 µm. H) Hippocampus with numerous RusV RNA signals in neurons of the granule cell layer in areas with or without irregular architecture. Scale bar indicates 50 µm. I) Cerebellum, no indication for inflammation or any degenerative process. Scale bar indicates 50 µm. J) Cerebellum with abundant RusV RNA labeling in Purkinje cells. Scale bar indicates 50 µm. A–C, E, G, I) Hematoxylin-eosin staining; D, F, H, I) RNAscope in situ hybridization with probes against the nonstructural protein–coding region of RusV, counterstained with Mayer's hematoxylin.

restricted to the gray matter but not affecting white matter or the cerebellar cortex (*1*,*4*,*5*). A similar syndrome was reported in cats from Alabama, USA, in 1979 but the etiology remained obscure (*7*). In Germany, RusV has been detected in a broad range of zoo animals with neurologic disorders, including lions (*Panthera leo*) (*8*–*11*).

Because initial diagnostic tests were negative in this case, and history, histopathology, and metatranscriptome sequencing suggested staggering disease, we sent tissue samples and sequence data from the mountain lion to the Friedrich-Loeffler-Institut (Greifswald-Insel Riems, Germany) for additional analyses. To demonstrate an association between the lesions and the virus, we used previously developed in situ hybridization methods for RusV (*1*,*6*) (Appendix), which demonstrated RusV RNA in all regions of the brain and nearly all levels of the spinal cord, irrespective of an inflammatory reaction. Only lumbosacral nerve roots (cauda equina) tested negative. RusV-specific RNA localized in neuronal cell bodies (Figure 1, panels D, F, H, J), disseminated within the neuropil of the gray matter (Figure 1, panel D, inlay) and, to a lesser extent, in the white matter. We found particularly abundant or large, dot-like signals in the granule cell layer of the hippocampus (Figure 1, panel H), and in Purkinje cells of the cerebellum (Figure 1, panel J), similar to findings from staggering disease cases in cats from Europe (*4*).

The overall architecture of the viral genome of the novel RusV from Colorado matched those of known RusV (Appendix Figure 2). The mean pairwise nucleotide identity between the novel RusV sequence and sequences from Germany was 69.9% and between sequences from Austria and Sweden was 68.9%; the sequences from Europe shared 76.7% identity among each other (Figure 2, panel A). The mean pairwise amino acid identities of the nonstructural and structural polyproteins ranged from 75.6% to 78.1% between the novel RusV sequence and the sequences from Europe (Figure 2, panel A). The genetic diversity was not equally distributed over the genome; part of the protease and the intergenic region showed especially high levels of sequence variations (Appendix Figure 2).

We performed phylogenetic analysis to compare the RusV sequence from Colorado with appropriate reference strains using an amino acid alignment of the structural polyprotein (Appendix). Those findings suggested classification of the novel RusV as a member of the family *Matonaviridae*, genus *Rubivirus*, placing it basal to the known RusV sequences detected in Germany, Sweden, and Austria (Figure 2, panel B). The basal position of the novel RusV in relation to all other known RusV is also supported by phylogeny based on the whole-genome nucleotide sequence (Appendix Figure 3).

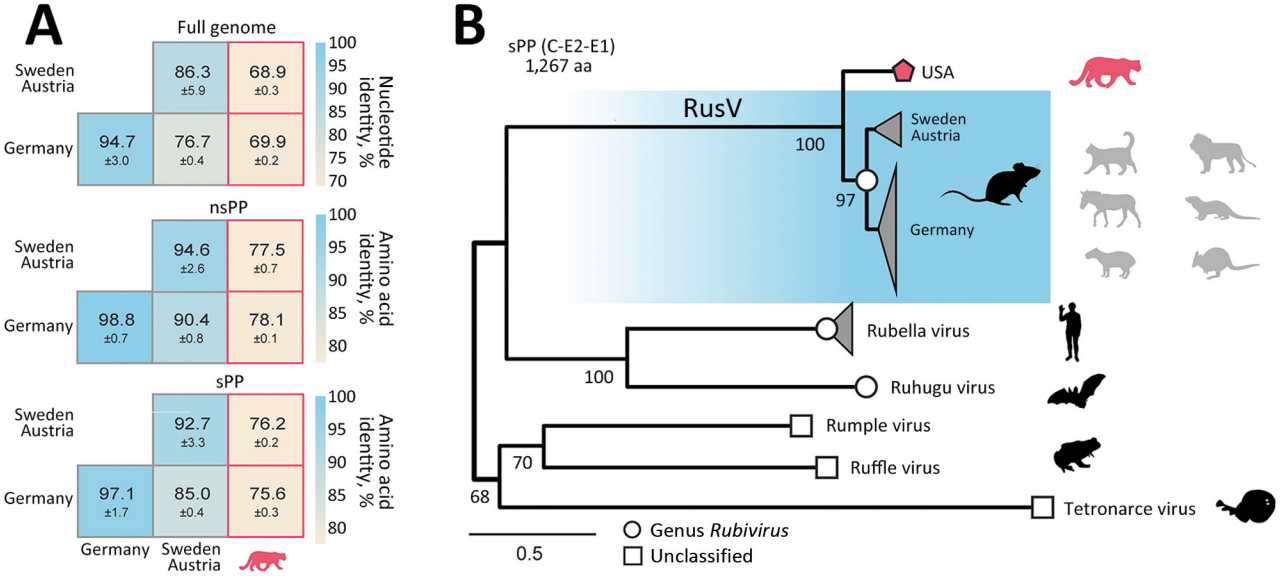

Figure 2. Sequence similarity and phylogenetic position of RusV in wild mountain lion (*Puma concolor*) with staggering disease, Colorado, USA. A) Mean pairwise sequence identity between the novel Colorado RusV and RusV sequences from Germany, Austria, and Sweden. Pairwise identity was based on nucleotide sequence alignments of the full genome or amino acid alignments of the nsPP and sPP. B) The sPP amino acid sequences of appropriate references from rubiviruses (circle) or currently unclassified matonavirids (square) were aligned with the novel RusV (pentagon). Phylogenetic tree was calculated using IQ-TREE (http://www.iqtree.org). Host species are depicted as silhouettes. For RusV, the potential reservoir (dark) and spillover hosts (light) are depicted. Scale bar indicates substitutions per site. nsPP, nonstructural polyprotein; sPP, structural polyprotein.

Conclusions

Our results demonstrate the presence of a RusV variant in North America that is divergent from those previously described from Europe. The clinical signs, histologic lesions, and infected target cells observed for the wild mountain lion in Colorado, USA, meet the case definition for staggering disease. A causative role for RusV is likely, further supporting previous work identifying RusV as the causative agent of staggering disease in domestic cats from Austria, Sweden, and Germany (*1*,*6*), and in lions from zoologic collections in Germany (*10*).

This report is limited to a single case of staggering disease in Colorado. To determine whether RusV is enzootic in this region, we recommend further investigations, including retrospective RusV testing of tissues from feline encephalitis cases of unknown causes in North America. Surveillance for RusV in small rodents might identify a local reservoir host because rodents of the genus *Apodemus* have been identified as likely RusV reservoir hosts in Europe through real-time reverse transcription PCR and sequencing of mice brain tissues (*1*,*8*,*9*,*12*,*13*). Although *Apodemus* mice are not indigenous to North America, several genera of small rodents are found throughout Colorado (*14*,*15*) and could serve as candidates for further screenings. In addition, future studies should consider that the zoonotic potential of RusV has not been determined.

Of note, a remarkably broad range of other mammalian RusV hosts has been identified in Germany, including equids, mustelids, rodents, and marsupials (*8*,*9*,*11*,*12*), raising concerns about a zoonotic potential of RusV (*8*,*9*). Given the wide host range of the virus in Europe, RusV should be considered as a possible cause for neurologic diseases in all mammal species in North America.

Acknowledgments

We thank Melanie Kaknes and Matt Martinez for submitting this case, Erica Rhinehart for providing video footage, Dan Tripp for advice on small mammal populations in Colorado, and Robin Brandt for pathology technical assistance.

About the Author

Dr. Fox is a veterinary anatomic pathologist at the Colorado State University Veterinary Diagnostic Laboratories. Her research interests include identification of emerging disease syndromes in Colorado wildlife and development of diagnostic strategies to inform wildlife management.

References

1. Matiasek K, Pfaff F, Weissenböck H, Wylezich C, Kolodziejek J, Tengstrand S, et al. Mystery of fatal 'staggering disease' unravelled: novel rustrela virus causes severe meningoencephalomyelitis in domestic cats. Nat Commun. 2023;14:624. https://doi.org/10.1038/s41467-023-36204-w
2. Lundgren A-L. Feline non-suppurative meningoencephalomyelitis. A clinical and pathological study. J Comp Pathol. 1992;107:411–25. https://doi.org/10.1016/0021-9975(92)90015-M
3. Kronevi T, Nordström M, Moreno W, Nilsson PO. Feline ataxia due to nonsuppurative meningoencephalomyelitis of unknown aetiology. Nord Vet Med. 1974;26:720–5.
4. Weissenböck H, Nowotny N, Zoher J. Feline meningoencephalomyelitis ("staggering disease") [in Austrian]. Wien Tierarztl Monatsschr. 1994;81:195–201.
5. Nowotny N, Weissenböck H. Description of feline nonsuppurative meningoencephalomyelitis ("staggering disease") and studies of its etiology. J Clin Microbiol. 1995;33:1668–9. https://doi.org/10.1128/jcm.33.6.1668-1669.1995
6. Weiss V, Weidinger P, Matt J, Weissenbacher-Lang C, Nowotny N, Weissenböck H. Rustrela virus-associated encephalomyelitis ('staggering disease') in cats from eastern Austria, 1994–2016. Viruses. 2023;15:1621. https://doi.org/10.3390/v15081621
7. Vandevelde M, Braund KG. Polioencephalomyelitis in cats. Vet Pathol. 1979;16:420–7. https://doi.org/10.1177/030098587901600404
8. Bennett AJ, Paskey AC, Ebinger A, Pfaff F, Priemer G, Höper D, et al. Author correction: relatives of rubella virus in diverse mammals. Nature. 2020;588:E2. https://doi.org/10.1038/s41586-020-2897-1
9. Bennett AJ, Paskey AC, Ebinger A, Pfaff F, Priemer G, Höper D, et al. Relatives of rubella virus in diverse mammals. Nature. 2020;586:424–8. https://doi.org/10.1038/s41586-020-2812-9
10. de le Roi M, Puff C, Wohlsein P, Pfaff F, Beer M, Baumgärtner W, et al. Rustrela virus as putative cause of nonsuppurative meningoencephalitis in lions. Emerg Infect Dis. 2023;29:1042–5. https://doi.org/10.3201/eid2905.230172
11. Voss A, Schlieben P, Gerst S, Wylezich C, Pfaff F, Langner C, et al. Rustrela virus infection—an emerging neuropathogen of red-necked wallabies (*Macropus rufogriseus*). Transbound Emerg Dis. 2022;69:4016–21. https://doi.org/10.1111/tbed.14708
12. Pfaff F, Breithaupt A, Rubbenstroth D, Nippert S, Baumbach C, Gerst S, et al. Revisiting rustrela virus: new cases of encephalitis and a solution to the capsid enigma. Microbiol Spectr. 2022;10:e0010322. https://doi.org/10.1128/spectrum.00103-22
13. Nippert S, Rubbenstroth D, Geers JA, Ebinger A, Hoffmann D, Breithaupt A, et al. Continuous presence of genetically diverse rustrela virus lineages in yellow-necked field mouse reservoir populations in northeastern Germany. Virus Evol. 2023;9:vead048. https://doi.org/10.1093/ve/vead048
14. Armstrong DM, Fitzgerald JP, Meaney CA. Mammals of Colorado. 2nd ed. Boulder (CO): University Press of Colorado; 2011.
15. Armstrong DM. Rocky Mountain Mammals. 3rd ed. Boulder (CO): University Press of Colorado; 2008.

Address for correspondence: Karen A. Fox, Colorado State University Veterinary Diagnostic Laboratories, 2450 Gillette Dr, 1644 Campus Delivery, Fort Collins, CO 80526, USA; email: 661karen.fox@colostate.edu

Article DOI: https://doi.org/10.3201/eid3008.240411

Rustrela Virus in Wild Mountain Lion (*Puma concolor*) with Staggering Disease, Colorado, USA

Appendix

Necropsy and Histopathology

Within three hours after euthanasia, the carcass was transported to a −20°C freezer and then thawed for postmortem examination 2 weeks after freezing. Tissues were preserved in 10% neutral buffered formalin for histologic examination. Tissues collected in formalin included brain, spinal cord, liver, spleen, lung, heart, kidney, stomach, duodenum, pancreas, jejunum, ileum, cecum, colon, ileocecal lymph node, tongue, haired skin, gluteal muscle, adrenal gland, and thyroid gland. Tissues collected and frozen for possible ancillary diagnostics included brain, spinal cord, retropharyngeal lymph node, liver, spleen, adipose tissue, stomach contents, and premolar. Formalin-fixed tissues were embedded in paraffin, sectioned at 5–6 μm, and sections examined by light microscopy after hematoxylin and eosin staining.

Diagnostic Testing for Encephalitic Pathogens

Initial diagnostics for encephalitic pathogens were conducted as shown in Appendix Table 1. All of these tests were performed as standard fee-for-service diagnostics by the Colorado State University Veterinary Diagnostic Laboratory. None of the targeted pathogens were detected by these tests.

Metatranscriptome Analysis

Tissues from pooled brain and spinal cord, targeting gray matter, were submitted for RNA extraction and metatranscriptome sequencing using an Illumina NovaSeq 6000 (2×150 bp)

through Novogene Research Services (Novogene, Beijing, China). The resulting raw sequence reads were initially trimmed using Trim Galore (v0.6.10; (*1*)) and Cutadapt (v 4.0; (*2*)) running in automated adaptor detection and paired-end mode. Trimmed raw reads were then de novo assembled using rnaSPAdes (v3.15.5; (*3*)) and Megahit (v1.2.9; (*4*)). The resulting contigs were then taxonomically classified using DIAMOND blastx (v2.1.8.162; (*5*)) against the non-redundant protein (nr) database from NCBI (version from Apr 2023; (*6*)). Contigs matching potential viral sequences were selected and checked using BLASTn (v2.13.0+; (*7*)) against the non-redundant nucleotide (nt) database from NCBI (version from Apr 2023; (*6*)).

Phylogenetic analysis

For a general taxonomic classification of the novel RusV sequence from a free-ranging mountain lion (Colorado, USA) the predicted amino acid sequence of the structural polyprotein (sPP) was selected for phylogenetic analysis as suggested by the ICTV study group (*8*). The sPP contains the mature peptides of the capsid and the two envelope glycoproteins E2 and E1. The amino acid sequence of sPP was then aligned with appropriate references from other rubiviruses or currently unclassified but related matonavirids from GenBank using MUSCLE (v3.8.425; (*9*)). The tree was constructed using IQ-TREE (version 2.2.3; (*10*)) using optimal model selection (*11*) and statistical support with 100.000 replicates each for ultrafast bootstrap (*12*) and SH-aLRT test.

For a more detailed analysis, the whole genome sequences of all available RusV entries available from GenBank (25.01.2024) were aligned along with the novel sequence using MAFFT (version 7.490; (*13*)). A phylogenetic tree was calculated as described above. The alignment was also used to calculate the mean genetic distance (K80 model) between the novel RusV sequence and the RusV sequences from Germany and Sweden/Austria using a sliding window (window: 400 nt, step size: 50 nt).

Nucleotide and amino acid identities were calculated between all pairs of available RusV whole genome sequences, and non-structural polyprotein (nsPP) and sPP, respectively. Mean pairwise identities were then calculated for RusV sequences from Germany and Sweden/Austria and compared to the novel RusV from USA.

PCR

Previously developed real-time reverse transcription PCR (RT-PCR) primers and probe (*14*) targeting the 5′ terminus of RusV were adapted for consensus sequence homology to the Colorado, USA mountain lion sequence and the European RusV sequences, as given in Appendix Table 2. RNA was extracted from a pooled sample of the suspect mountain lion brain and spinal cord, targeting gray matter, using an Allprep Power Viral DNA/RNA kit (Qiagen, Germantown, MD) and DNase Max kit (Qiagen) according to manufacturer's instructions. We used a TaqMan Fast Virus 1-Step Master Mix (Thermo Fisher Scientific, Waltham, MA), and VetMAX Xeno Internal Positive Control-VIC Assay with VetMAX Xeno Internal Positive Control RNA (Thermo Fisher Scientific) according to manufacturer's instructions. We used 5.0 µL of extracted template RNA in a total reaction volume of 25 µL. Reactions were cycled using an Eco real-time PCR thermocycler (Illumina, San Diego, CA) and Eco software (Illumina, v. 4.0.07.0) for analysis. Automated thresholds were used due to lack of known positive control material for standard curve dilutions in Colorado, USA. Negative controls (normal mountain lion pooled brain and spinal cord, and no template control) and internal positive RNA controls were adequate for interpretation.

In situ Hybridization

In situ hybridization for the detection of RusV RNA in brain and spinal cord tissue sections was performed with the RNAScope 2–5 HD Reagent Kit-Red (Advanced Cell Diagnostics) according to the manufacturer's instructions. Probes were custom-designed for the non-structural protein gene of the sequence obtained from the puma brain (Catalog number 1323611-C1). As technical assay controls, a positive control probe (*Felis catus* peptidylprolyl isomerase B, *PPIB*) and a negative control probe (dihydrodipicolinate reductase) were included. Archived brain tissue slides from a snow leopard (*Panthera uncia*) diagnosed with ocular, bilateral anterior segment dysgenesis were included as negative controls. All slides were scanned using a Hamamatsu S60 scanner, evaluation was done using the NDPview.2 plus software (Version 2.8.24, Hamamatsu Photonics, K.K. Japan). Interpretation was performed by a board-certified pathologist (DiplECVP). Representative photographs of control slides are shown in Appendix Figure 4.

References

1. Krueger F. 2023. Trim Galore. https://www.bioinformatics.babraham.ac.uk/projects/trim_galore

2. Martin M. Cutadapt removes adapter sequences from high-throughput sequencing reads. EMBnet J. 2011;17:10. https://doi.org/10.14806/ej.17.1.200

3. Bushmanova E, Antipov D, Lapidus A, Prjibelski AD. rnaSPAdes: a de novo transcriptome assembler and its application to RNA-Seq data. Gigascience. 2019;8:8. PubMed https://doi.org/10.1093/gigascience/giz100

4. Li D, Liu C-M, Luo R, Sadakane K, Lam T-W. MEGAHIT: an ultra-fast single-node solution for large and complex metagenomics assembly via succinct de Bruijn graph. Bioinformatics. 2015;31:1674–6. PubMed https://doi.org/10.1093/bioinformatics/btv033

5. Buchfink B, Reuter K, Drost H-G. Sensitive protein alignments at tree-of-life scale using DIAMOND. Nat Methods. 2021;18:366–8. PubMed https://doi.org/10.1038/s41592-021-01101-x

6. Sayers EW, Bolton EE, Brister JR, Canese K, Chan J, Comeau DC, et al. Database resources of the national center for biotechnology information. Nucleic Acids Res. 2022;50(D1):D20–6. PubMed https://doi.org/10.1093/nar/gkab1112

7. Camacho C, Coulouris G, Avagyan V, Ma N, Papadopoulos J, Bealer K, et al. BLAST+: architecture and applications. BMC Bioinformatics. 2009;10:421. PubMed https://doi.org/10.1186/1471-2105-10-421

8. Mankertz A, Chen M-H, Goldberg TL, Hübschen JM, Pfaff F, Ulrich RG; Ictv Report Consortium. ICTV Virus Taxonomy Profile: *Matonaviridae* 2022. J Gen Virol. 2022;103:103. PubMed https://doi.org/10.1099/jgv.0.001817

9. Edgar RC. MUSCLE: multiple sequence alignment with high accuracy and high throughput. Nucleic Acids Res. 2004;32:1792–7. PubMed https://doi.org/10.1093/nar/gkh340

10. Minh BQ, Schmidt HA, Chernomor O, Schrempf D, Woodhams MD, von Haeseler A, et al. IQ-TREE 2: new models and efficient methods for phylogenetic inference in the genomic era. Mol Biol Evol. 2020;37:1530–4. PubMed https://doi.org/10.1093/molbev/msaa015

11. Kalyaanamoorthy S, Minh BQ, Wong TKF, von Haeseler A, Jermiin LS. ModelFinder: fast model selection for accurate phylogenetic estimates. Nat Methods. 2017;14:587–9. PubMed https://doi.org/10.1038/nmeth.4285

12. Hoang DT, Chernomor O, von Haeseler A, Minh BQ, Vinh LS. UFBoot2: improving the ultrafast bootstrap approximation. Mol Biol Evol. 2018;35:518–22. PubMed https://doi.org/10.1093/molbev/msx281

13. Katoh K, Misawa K, Kuma K, Miyata T. MAFFT: a novel method for rapid multiple sequence alignment based on fast Fourier transform. Nucleic Acids Res. 2002;30:3059–66. PubMed https://doi.org/10.1093/nar/gkf436

14. Matiasek K, Pfaff F, Weissenböck H, Wylezich C, Kolodziejek J, Tengstrand S, et al. Mystery of fatal 'staggering disease' unravelled: novel rustrela virus causes severe meningoencephalomyelitis in domestic cats. Nat Commun. 2023;14:624. PubMed https://doi.org/10.1038/s41467-023-36204-w

Appendix Table 1. Initial diagnostics performed to investigate differential diagnoses for meningoecephalomyelitis in a free-ranging mountain lion*

Targeted pathogen	Test	Tissue	Result
Feline panleukopenia virus	Real-time RT-PCR	Brain	Not detected
Canine distemper virus	Real-time RT-PCR	Brain	Not detected
West Nile virus	Real-time RT-PCR	Brain	Not detected
Toxoplasma gondii	PCR	Brain	Not detected
Influenza A virus	Real-time RT-PCR	Spinal cord	Not detected
Rabies virus	Immunofluorescence	Brainstem	Not detected
Feline coronavirus (feline infectious peritonitis)	Immunohistochemistry	Brain (cerebral cortex)	Not detected

*RT-PCR, reverse transcription PCR.

Appendix Table 2. Real-time RT-PCR assay details, with primers and probe adapted for consensus homology to the Colorado, USA mountain lion RusV sequence and European sequences*

Primer/Probe/Condition	Details
RusV_234 (fw) adapted primer	CCCYGTGTTCCTAGGCAC; 0.8 µM
RusV_323 (rv) adapted primer	TCGCCCCATTCDACCCAATT; 0.8 µM
RusV_256 adapted probe	GTGMGCGACCACCCAGCACTCCA; 0.4 µM
Probe modifications	5′FAM/ZEN/3′IBFQ
VetMAX Xeno IPC RNA	2 µL added to samples before lysis
VetMAX Xeno IPC-VIC assay	1 µL added to 25 µL PCR reaction mix
Cycling conditions	45°C × 10 min
	95°C × 10 min
	45 cycles of:
	95°C × 15 s
	60°C × 30 s
	72°C × 30 s

*Adapted from (*14*).

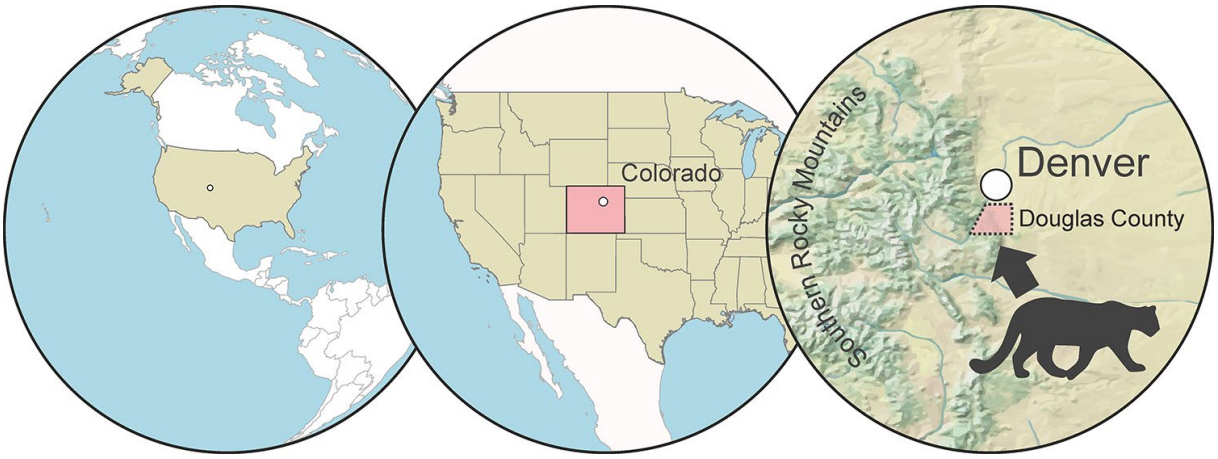

Appendix Figure 1. The free-ranging mountain lion (*Puma concolor*) was found in a residential area of Douglas County which is located south of Denver (Colorado, USA). Made with Natural Earth.

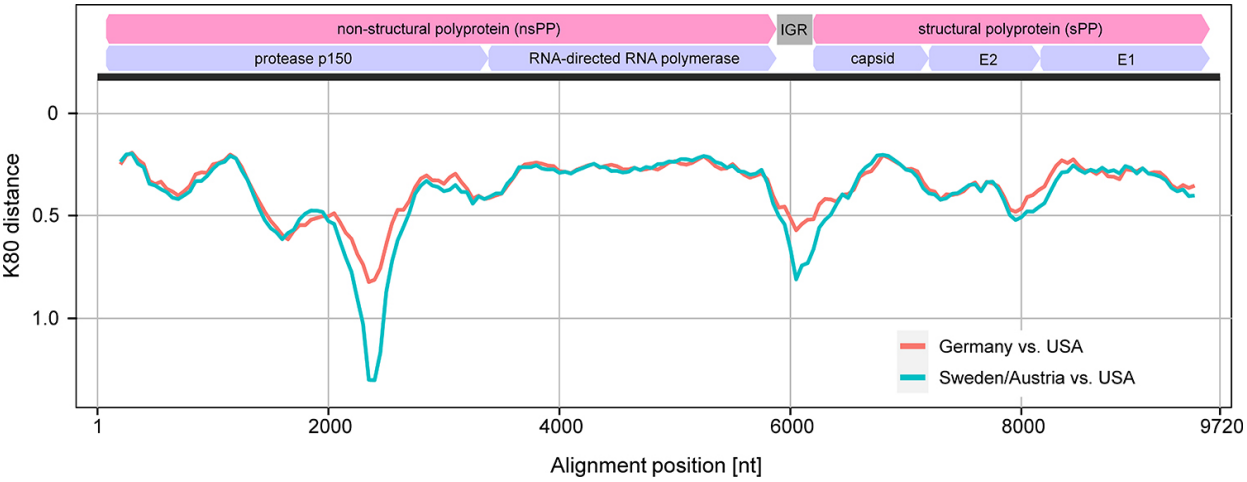

Appendix Figure 2. The mean genetic distance (K80 model) between the novel RusV sequence from a free-ranging mountain lion from Colorado, USA, and the published RusV sequences from Germany or Sweden/Austria was calculated in a sliding window (window: 400 nt, step size: 50 nt) based on a whole genome nucleotide alignment (9,720 nt). The genomic architecture of RusV (deduced from MN552442.2) is shown: pink arrows represent ORFs that encode the polyproteins nsPP and sPP, while blue arrows represent mature peptides that are produced by cleavage from the polyproteins. The intergenic region (IGR) is located between both nsPP and sPP.

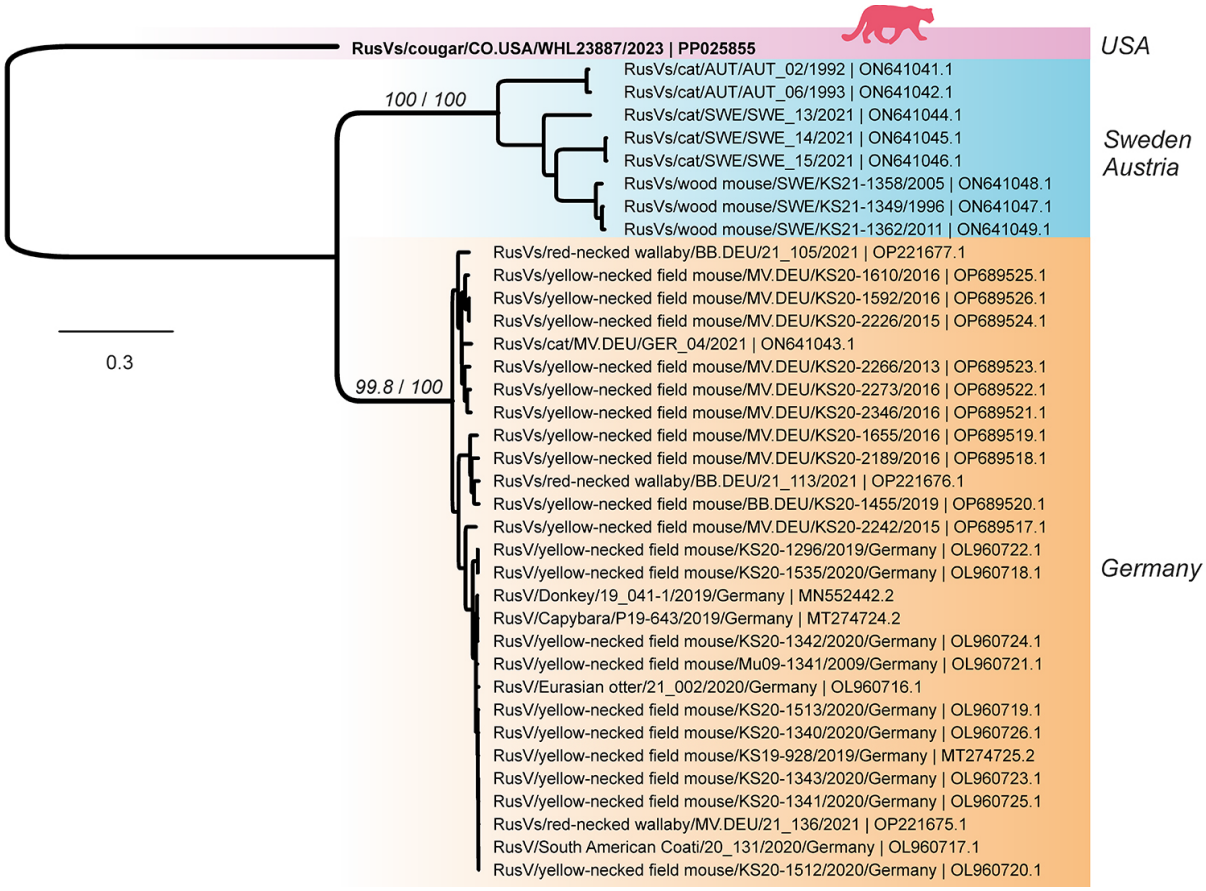

Appendix Figure 3. Phylogenetic position of rustrela virus (RusV) based on a nucleotide alignment of whole genomes (9,720 nt). The novel RusV sequence from a free-ranging mountain lion from Colorado, USA is highlighted using bold text. RusV genetic groups are highlighted and labeled according to their geographic origin. Alignment was done using MAFFT (version 7.490; (*13*)). The tree was constructed using IQ-TREE (version 2.2.3; (*10*)) using optimal model selection and statistical support with 100.000 replicates each for ultrafast bootstrap (*12*) and SH-aLRT test. Statistical support is shown for main branches using the format [ultrafast bootstrap/SH-aLRT]. Scale bar indicates nucleotide substitutions per site.

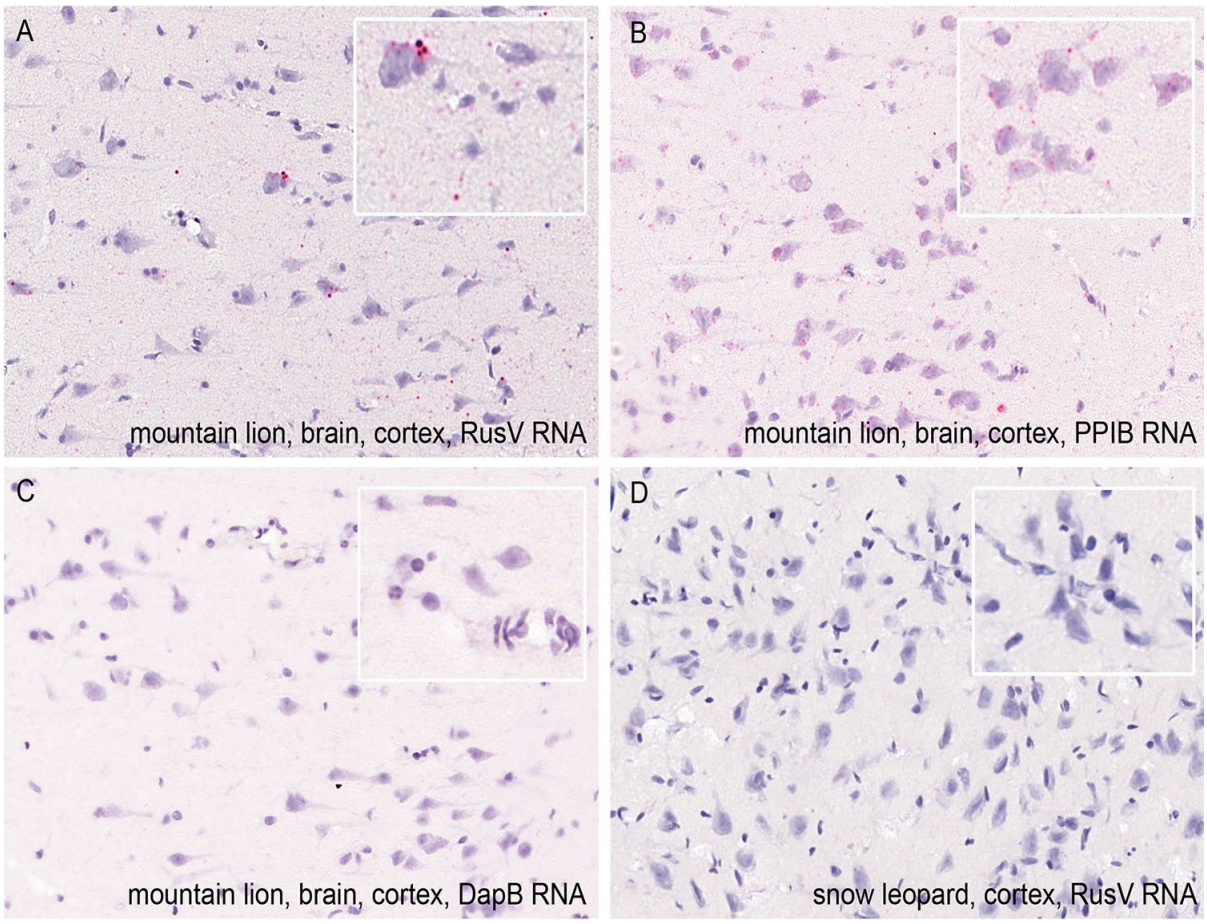

Appendix Figure 4. RNA in situ hybridization for rustrela virus (RusV) RNA detection in brain tissues including controls. A) Chromogenic labeling (fast red) with probes against the NSP-coding region of RusV, visible in in cortical neurons and in the neuropil of the mountain lion. B) Technical, positive control probe (*Felis catus*) peptidylprolyl isomerase B, *PPIB* yielding disseminated labeling. C) Technical negative control probe (dihydrodipicolinate reductase, *DapB*) showing no labeling. D) Archived brain tissue slides from a snow leopard (*Panthera uncia*) tested negative for RusV-RNA. All slides counterstained with Mayer's hematoxylin counterstain, inlays show higher magnifications.